INFLUENCES OF WELDING PROCESSES AND POST-WELD AGEING TREATMENT ON MECHANICAL AND METALLURGICAL PROPERTIES OF AA2219 ALUMINIUM ALLOY JOINTS

S. Malarvizhi and V. Balasubramanian

ABSTRACT

AA2219 aluminium alloy joints without filler metal addition were fabricated using gas tungsten arc welding (GTAW), electron beam welding (EBW) and friction stir welding (FSW) processes. The fabricated joints were post weld aged at 175 °C for 12 h. Microstructure analysis was carried out using optical and electron microscopes. It was found that the FSW joints were exhibiting superior tensile and fatigue properties compared to EBW and GTAW joints. Post-weld ageing treatment was found to be beneficial to enhance the tensile and fatigue properties of the welded joints, irrespective of welding processes. Post weld aged FSW joints showed the highest joint efficiency of 80 % and hence this process can be preferred over other welding processes to fabricate components and structures using AA2219 aluminium alloys.

IIW-Thesaurus keywords: *Aluminium alloy; Gas tungsten; Arc welding; Electron beam welding; Friction stir welding; Post weld; Ageing; Treatment; Tensile properties.*

1 Introduction

Aluminium alloy 2219 (Al-Cu-Mn ternary alloy) has excellent cryogenic properties. It has a unique combination of properties such as good weldability, high strength to weight ratio. The preferred welding processes for AA2219 aluminium alloy are frequently gas metal arc welding (GMAW) and gas tungsten arc welding (GTAW) due to their comparatively easier applicability and better economy [1]. Plasma arc welding (PAW) with a positive polarity electrode and high welding current allows aluminium components to be joined economically with an excellent weld quality [2]. In comparison with the electric arcs, the electron beam is characterized by a higher power density and thus permits the single pass welding of square butt joints with thickness up to approximately 8 mm in the flat position at welding speeds up to more than 1 m/min. The electron beam welds of most of the weldable materials including aluminium alloys exhibit superior mechanical properties compared to the welds made using GTAW [3]. Application of GMAW process to weld AA2219 aluminium alloy is not preferred due to the non-availability of matching filler wires. Similarly application of laser beam welding (LBW) process to weld AA2219 aluminium ally is also not preferred due to low energy efficiency of the process due to high reflectivity of aluminium alloys [4].

Though AA2219 has got an edge over its 6000 and 7000 series counterparts in terms of weldability, it also suffers from poor as-welded joint strength. This is true both in autogenous welds as well as those welded with the matching filler. The loss of strength is due to the melting and quick resolidification, which renders all the strengthening precipitates to dissolve and the material is as good as a cast material with solute segregation and large columnar grains [5]. Compared to many of the fusion welding processes that are routinely used for joining structural alloys, friction stir welding (FSW) is an emerging solid state joining process in which the material that is being welded does not melt and recast [6]. Also, friction stir welding process is finding wide applications in joining most of the aluminium alloys. FSW process is observed to offer several advantages over fusion welding due to the absence of parent metal melting. During welding, the frictional heat associated with the thermal cycle varies in transverse direction of the weld. Maximum temperature is observed in the stirzone, which causes alteration in

Doc. IIW-2303 recommended for publication by Commission IX "Behaviour of Metals Subjected to Welding."

the precipitate distribution present in the base material and also due to stirring of the plasticized material. These changes in the heat and temperature distribution in welding process alter the strength and ductility of the joints [7].

The gap between strength values of the base metal and weld metal, particularly yield strength values, is significantly large, forcing the design engineers to use thicker base metal plates, which in turn increases the total weight of the structure. This fact is of concern in aerospace applications because, use of thicker plates due to low yield strength of the weld metal results in lowering of the payload [8]. If the yield strength of the weld metal can be increased by some means it will be of advantage.

Liu *et al.* [9] investigated the effect of zigzag line on the mechanical properties of friction stir welded joints of AA2219-O aluminium alloy. They found that the zigzag line has no effect on the mechanical properties of the as-welded joint but seriously deteriorates those of the heat treated joint. Weifeng Xu *et al.* [10] have investigated the microstructure, second phase particles and mechanical properties of friction stir welded joints of AA2219-T6 aluminium alloy. They observed that the tensile strength, yield strength, elongation and joint efficiency of joints presented a sharp decline after a peak value with increasing rotary speed from 800 rpm to 1 300 rpm. Bala Srinivasan *et al.* [11] characterized friction stir weldment of AA2219-T87 aluminium alloy for its microstructure, mechanical properties and corrosion resistance and stress corrosion cracking behaviour. They reported that the dissolution and coarsening of the strengthening precipitates in the weld nugget had resulted in the softening of these regions; nevertheless, the weld joint was found to have an efficiency of around 72 %.

2 Objectives

From the literature review, it is understood that the mechanical and metallurgical properties of GTAW, EBW and FSW joints of AA2219 aluminium alloy were investigated by many researchers individually but nobody has attempted to compare the properties of these joints combinedly. The influence of post-weld ageing treatment on mechanical and metallurgical properties of these joints was not yet compared. Hence, an attempt was made to compare the tensile and fatigue properties of as-welded and post weld aged GTAW, EBW and FSW joints of AA2219 aluminium alloy.

3 Experimental work

The rolled plates of AA2219-T87 aluminium alloy were cut and machined to the required sizes (300 mm × 150 mm × 5 mm) by power hacksaw cutting and grinding. The chemical composition and mechanical properties of base metal are given in Tables 1 and 2, respectively.

Square butt joint configuration, as shown in Figure 1 a) was prepared to fabricate GTAW, EBW and FSW joints without filler metal additions. GTAW joints were fabricated using Tungsten Inert Gas welding machine (Lincoln, USA) with 400 A capacity. EBW joints were fabricated using an Electron Beam welding machine (Techmeta, France) with 100 kV capacity. FSW joints were fabricated using computer controlled friction stir welding machine (RV Machine Tools, India) with a non-consumable high carbon steel tool. Large numbers of trial experiments were conducted to optimise the welding conditions. The trial which produced a joint with full penetration and free from macro level defects was taken as optimized welding conditions. The optimised conditions used to weld the joints are presented in Table 3.

Mechanical and metallurgical properties of the joints were evaluated immediately after the fabrication of joints, without giving any heat treatment, to obtain as-welded (AW) joint properties. Post-weld ageing (PWA) treatment was carried out at 175 °C for a soaking period of 12 h. Joints were placed into the induction furnace and heated from room temperature to the soaking temperature at a rate of 100 °C per hour. After completion of the soaking period, the joints were cooled down in the furnace to room temperature.

The joints were sliced using power hacksaw and then machined to the required dimensions. Two types of tensile test specimens, smooth unnotched [Figure 1 b)] and notched specimens [Figure 1 c)] were prepared as per the ASTM E8M-04 specification. Tensile test was carried out in 100 kN, electro-mechanical controlled Universal Testing Machine (Make: FIE, India, Model: UNITECH

Table 1 – Chemical composition [wt. %] of base metal

Type of Material	Cu	Mn	Fe	Zr	V	Si	Ti	Zn	Al
Base metal (AA 2219-T87)	6.33	0.34	0.13	0.12	0.07	0.06	0.04	0.02	Bal

Table 2 – Mechanical properties of base metal

Yield strength [MPa]	Ultimate tensile strength [MPa]	Elongation [%]	Reduction in cross-sectional area [%]	Vickers hardness (0.05 kg for 15 s), VHN
392	475	15	10	140

Table 3 – Welding conditions and process parameters

Parameter	GTAW	EBW	FSW
Current	150 A	51 mA	
Voltage	30 V	50 kV	
Welding speed	3 mm/s	16 mm/s	1.5 mm/s
Polarity	AC	DC	--
Vacuum	--	10^{-4} bar	
Shielding gas	99.99 % pure argon	--	--
Gas flow rate	14 l/min	--	--
Tool rotational speed			1400 rpm
Axial force			12 kN
FSW tool details			Threaded pin with 6 mm diameter and 4.8 mm length made of high carbon steel

94001). The 0.2 % offset yield strength, ultimate tensile strength, percentage of elongation and joint efficiency were recorded from unnotched specimen. Notch tensile strength and notch strength ratio were evaluated using notched specimen. Scanning electron microscope (Make: JEOL Japan, Model: 5610LV) at higher magnification was used to study the fracture morphology of tensile tested specimens to establish the nature of the fracture. Fracture surfaces were preserved by coating with commercial oxide proof oil. Before examining, the specimens were cleaned ultrasonically with carbon tetrachloride and acetone.

Unnotched fatigue specimens were prepared as shown in Figure 1 b) from welded joints in the transverse direction (normal to the welding direction) to evaluate the fatigue life. Notched fatigue specimens were also prepared as shown in Figure 1 c) from welded joints to evaluate the fatigue notch factor and notch sensitivity factor. The fatigue testing experiment were conducted at five different stress levels. All the experiments were conducted under uniaxial tensile loading condition (stress ratio = 0) using servo hydraulic fatigue testing machine (Make: INSTRON, UK; Model: 8801). At each stress levels three specimens were tested and the average of the test results are used to plot S-N curves.

Vicker's microhardness testing machine (Make: Matzusawa, Japan, Model: MMT-X7) was employed for measuring the hardness across the joint with 0.05 kg load for 15 s. Microstructural analysis was carried out using

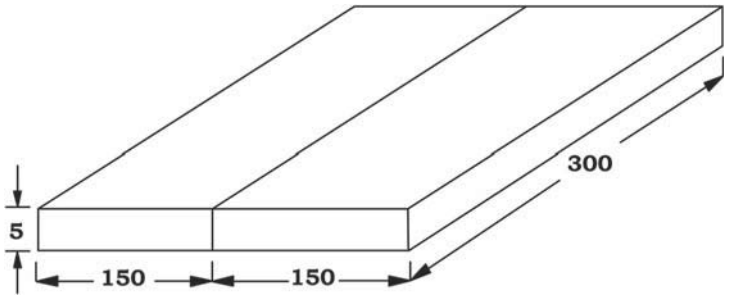

a) Dimensions of square butt joints

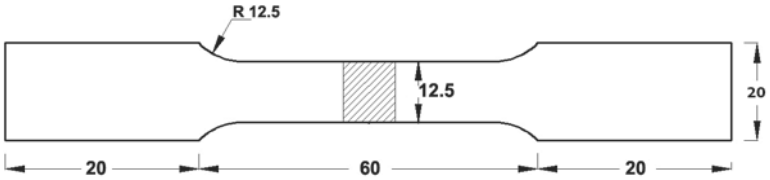

b) Unnotched fatigue/tensile specimen

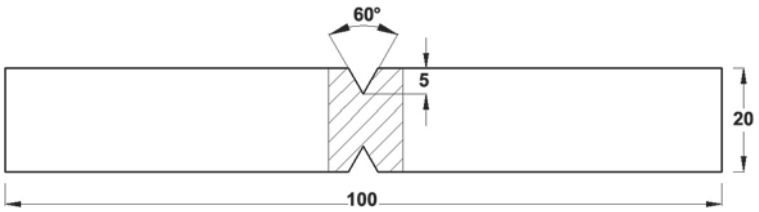

c) Notched fatigue/tensile specimen

Figure 1 – Configuration of joint and test specimen

a light optical microscope (Make: MEIJI, Japan, Model: ML7100) incorporated with an image analyzing software (Metal Vision). The specimens for microstructural analysis were sectioned to the required sizes from the joint comprising weld metal, HAZ and base metal regions and were polished using different grades of emery papers. Final polishing was done using the diamond compound (1 µm particle size) in the disc-polishing machine. Specimens were etched with Kellers reagent to reveal the microstructure. Since most of the joints failed in the weld metal, the weld metal of the joints alone were analysed using transmission electron microscope (Make: PHILIPS, Model: CM20) to get more information about size of the precipitates and distribution of precipitates. Electron dispersive X-ray (EDX) analysis was also undertaken to find the composition of the specific precipitates.

4 Results

4.1 Tensile properties

The experimentally evaluated transverse tensile properties of as-welded (AW) and post weld aged (PWA) joints are presented in Tables 4 and 5 respectively. All the values are average of three results. The unwelded parent metal showed a yield strength and tensile strength of 392 MPa and 475 MPa. Of the three welded joints, the GTAW joints showed the lowest yield strength and tensile strength of 220 MPa and 242 MPa. This suggests that there is a 50 % reduction in strength values due to GTA welding. FSW joints showed the highest yield strength and tensile strength of 305 MPa and 342 MPa. Though these values are lower than the base metal, the strength values are 40 % higher than GTAW joints. EBW joints showed the yield strength and tensile strength of 265 MPa and 304 MPa, which is 30 % higher than GTAW joints but 15 % lower than FSW joints.

The unwelded parent metal showed an elongation and reduction in cross sectional area (c.s.a.) of 15 % and 10 %. Of the three welded joints, the GTAW joints showed the lowest elongation and reduction in cross sectional area of 8.8 % and 6.2 %. This suggests that there is a 40 % reduction in ductility values due to GTA welding. FSW joints showed the highest elongation and reduction in cross sectional area of 12.2 % and 8.6 %. Though these values are lower than the base metal, the ductility values are 40 % higher than GTAW joints. EBW joints also showed an elongation and reduction in cross sectional area of 10.4 % and 7.5 %, which is 20 % higher than GTAW joints but 15 % lower than FSW joints.

Notch strength ratio (NSR) is the ratio between tensile strength of notched specimen and tensile strength of unnotched specimen. It is found to be less than unity (<1) for base metal and welded joints of AA2219 aluminium alloy. From these results, it is inferred that the AA2219 alloy is sensitive to notches and they fall into the 'notch brittle materials' category. Of the three welded joints, FSW joints showed highest NSR of 0.85 (sensitivity to notches is lower) and GTAW joints showed lowest NSR of 0.75 (sensitivity to notches is higher). Of the three welded joints, the FSW joints showed the highest joint efficiency of 72 % which is 20 % higher than GTAW joints and 12 % higher than EBW joints. All the joints showed approximately 10 % enhancement in the values due to the post-weld ageing and this is evident from the results presented in Table 5.

4.2 Fatigue properties

Figures 2 a) and 2 b) show the fatigue life of as-welded and post weld aged unnotched specimens in the form of S-N curves. The effect of welding processes and post-weld ageing treatment on fatigue life of the joints is revealed by these figures. The S-N curve in the high cycle fatigue region is represented by the Basquin equation [12]

Table 4 – Transverse tensile properties of as-welded (AW) joints

Joint type	Yield strength [MPa]	Ultimate tensile strength [MPa]	Elongation [%]	Reduction in cross sectional area [%]	Notch tensile strength [MPa]	Notch strength ratio (NSR)	Joint efficiency [%]
BM	392	475	15.0	10.0	442	0.93	---
GTAW	220	242	8.8	6.2	182	0.75	51
EBW	265	304	10.4	7.5	243	0.80	64
FSW	305	342	12.2	8.6	291	0.85	72

Table 5 – Transverse tensile properties of post weld aged (PWA) joints

Joint type	Yield strength [MPa]	Ultimate tensile strength [MPa]	Elongation [%]	Reduction in cross sectional area [%]	Notch tensile strength [MPa]	Notch strength ratio (NSR)	Joint efficiency [%]
BM	392	475	15.0	10.0	442	0.93	---
GTAW	237	266	9.6	6.8	213	0.80	56
EBW	300	330	11.8	8.3	280	0.85	70
FSW	344	382	13.2	9.1	343	0.90	80

$S^n N = A$ (1)

where

S is the stress amplitude,

N is the number of cycles to failure and,

n and A are empirical constants.

Each S-N curve shown in Figure 2 can be represented by the above equation. From those equations, the empirical constants n (slope of the curve) and A (intercept of the curve) were evaluated and they are presented in Tables 3 and 4.

When comparing the fatigue strength of different welded joints subjected to similar loading, it is convenient to express fatigue strength in terms of the stresses corresponding to particular lives, for example 10^5, 10^6 and 10^7 cycles on the mean S-N curve. The choice of reference life is quite arbitrary, 2×10^6 cycles has been used, and indeed some design codes refer to their S-N curves in terms of the corresponding stress range [13, 14]. For these reasons, in this investigation, applied stress range on the welded specimen at 2×10^6 cycles was taken as fatigue strength for comparison. The fatigue strength was evaluated for all the joints and they are presented in Tables 6 and 7.

The fatigue strength of unwelded AA2219 aluminium alloy is 200 MPa. All the three welding processes are found to be detrimental on fatigue strength of AA2219 aluminium alloy and it is clearly evident from Figure 2 a). Of the three as-welded (AW) joints, the joints fabricated by FSW process exhibited very high fatigue strength values. The fatigue strength of FSW joint is 175 MPa and it is 10 % lower (with respect to stress at 2 x 10^6 cycles) compared to the fatigue strength of base metal. EBW joint shows fatigue strength of 150 MPa which is 25 % lower than the base metal. GTAW joint shows the lowest fatigue strength of 110 MPa which is 45 % lower than the base metal. The introduction of notch will alter the stress distribution at the vicinity of notch and the stress value will be magnified nearer to the tip of the notch and this will have a definite effect on fatigue life of the components [15]. Hence, in this investigation, fatigue notch factor and notch sensitivity factor were calculated to evaluate the effect of notches on fatigue life of welded joints. The effect of notches on fatigue strength was determined by comparing the S-N curves of notched and unnotched specimens. The data for notched specimens were usually plotted [Figure 2 b)] in terms of nominal stress based on the net section of the specimen. The effectiveness of the

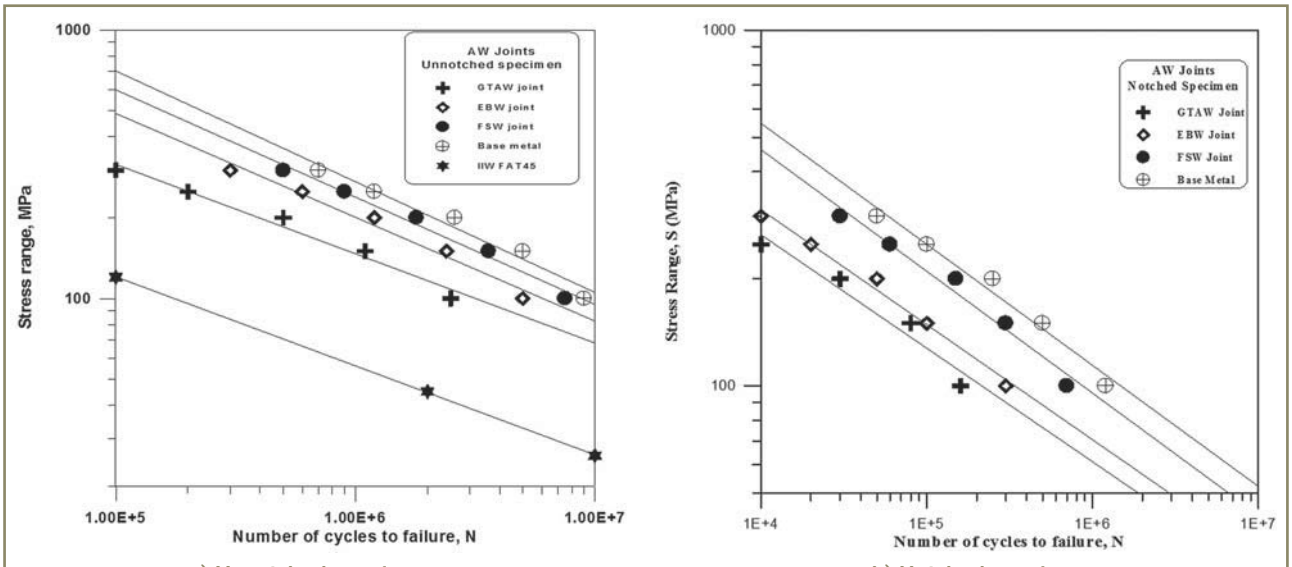

Figure 2 – S-N curves of as-welded (AW) joints

Table 6 – Fatigue properties of as-welded (AW) joints

Joint type	Slope of the S-N curve n	Intercept of the S-N curve A	Fatigue strength of unnotched specimens at 2×10^6 cycles [MPa]	Fatigue strength of notch specimens at 2×10^6 cycles [MPa]	Fatigue notch factor K_f	Notch sensitivity factor q
Base metal	-2.38	2.1×10^{10}	200	110	1.82	0.33
GTAW	- 3.03	2.2×10^9	110	50	3.21	0.75
EBW	-2.77	6.3×10^9	150	55	2.73	0.69
FSW	-2.56	9.1×10^9	180	80	2.19	0.48

Table 7 – Fatigue properties of post weld aged (PWA) joints

Joint Type	Slope of the S-N curve n	Intercept of the S-N curve A	Fatigue strength of unnotched specimens at 2 x 10^6 cycles [MPa]	Fatigue strength of notch specimens at 2 x 10^6 cycles [MPa]	Fatigue notch factor K_f	Notch sensitivity factor q
Base Metal	-2.38	2.1×10^{10}	200	110	1.82	0.33
GTAW	-2.85	2.8×10^{9}	120	60	2.95	0.61
EBW	-2.56	6.7×10^{9}	170	70	2.19	0.48
FSW	-2.43	9.6×10^{9}	190	90	1.90	0.36

notch in decreasing the fatigue strength was expressed by the fatigue strength reduction factor or fatigue notch factor, K_f. The fatigue notch factor for all the joints was evaluated using the following expression [15] and they are given in Tables 6 and 7.

K_f = Fatigue strength of unnotched specimen / Fatigue strength of notched specimen (2)

The notch sensitivity of material fatigue strength in fatigue is expressed by a notch sensitivity factor 'q' and it can be evaluated using the following expression [16]

$$q = (K_f - 1) / (K_t - 1) \quad (3)$$

where

K_t is the theoretical stress concentration factor and is the ratio of maximum stress to nominal stress. Using the above expression fatigue notch sensitivity factor q was evaluated for all the joints and they are presented in Tables 6 and 7. The fatigue notch factor of unwelded AA2219 aluminium alloy is 1.82. But the fatigue notch factor of as-welded (AW) joint is 2.73. Of the three as-welded (AW) joints, the FSW joint exhibits very low fatigue notch factor value and the GTAW joint shows very high fatigue notch factor value. Similar trend is observed in notch sensitivity factor values also since it is derived using fatigue notch factor values.

The SN curves for post weld aged (PWA) joints are displayed in Figure 3. Of the three PWA joints, the FSW joint exhibits very high fatigue strength values. The fatigue strength of post weld aged FSW joint is 190 MPa and it is 10 % higher compared to the fatigue strength of as-welded FSW joint. The fatigue strength of post weld aged EBW joint is 170 MPa which is 12 % higher than the as-welded EBW joint. The post weld aged GTAW joint shows the lowest fatigue strength of 120 MPa which is 10 % higher than the as-welded GTAW joint. Slope of the S-N curve is another measure to understand the fatigue performance of welded joints. If the slope of the S-N curve is larger, then the fatigue life will be higher and vice versa [17]. The unwelded parent metal shows the highest slope and the GTAW joint shows the lowest slope under as-welded and post weld aged conditions. The post-weld ageing (PWA) treatment is found to be beneficial to reduce the severity of notches under fatigue loading. Generally, if the fatigue notch factor is lower, then the fatigue life of the joints will be higher and vice versa [15].

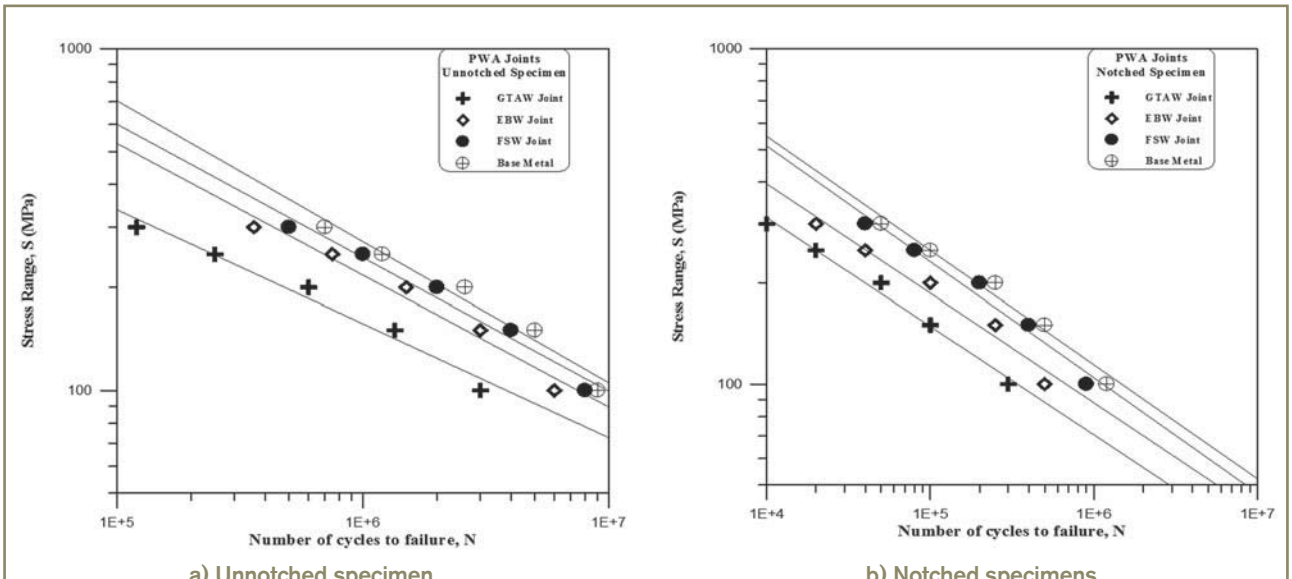

a) Unnotched specimen

b) Notched specimens

Figure 3 – S-N curves of post weld aged (PWA) Joints

4.3 Weld metal hardness

All the specimens invariably failed at weld metal under tensile and fatigue loading and hence microhardness is measured at the mid cross-section of weld metal and the hardness values are presented in Table 8. The base metal (unwelded parent metal) in its initial T_{87} condition showed a hardness value of 140 HV. The hardness is greatly reduced in the weld metal, irrespective of welding processes. This is one of the reasons for the location of failure at the weld metal. GTAW joint showed the lowest hardness of 90 HV at weld metal. This suggests that the hardness is reduced by 50 HV in the weld metal due to welding heat. FSW joint showed highest hardness of 110 HV at the weld nugget. Though this value is much lower than the base metal, it is 20 HV higher than GTAW joint and 5 HV higher than EBW joint. The post-weld ageing treatment increased the hardness of the weld metal from 10 to 14 HV for all the joints.

4.4 Microstructure

The macrostructure taken at the cross section of welded joints are presented in Figure 4. Optical micrographs of weld metal of the joints are displayed in Figure 5. The weld metal of GTAW joint shows coarse and elongated grains normal to the welding direction [Figures 5 a) and b)]. The weld metal of EBW joint contains very fine grains than GTAW joint [Figures 5 c) and d)]. The weld metal of FSW joint contains finer grains [Figures 5 e) and f)] compared to GTAW and EBW joints. However, the size and distribution of strengthening precipitates are not seen clearly in the optical micrographs and hence, the weld metal of the joints were analysed using TEM (Transmission Electron Microscope).

In as-welded GTAW joint, the precipitates are completely dissolved in the matrix and very few particles are seen [Figure 6 a)]. The weld metal of as-welded EBW joint experiences a fast cooling rate and the resulting material is like that of solutionized material [Figure 6 b)] with very less amount of undissolved precipitates. In as-welded FSW joint, the particles are fine and uniformly distributed throughout the matrix [Figure 6 c)]. The weld metal of post weld aged joints [Figures 6 d) to f)] contains more amount of precipitates than as-welded joints, irrespective of welding processes.

Electron Dispersive Analysis of XRays (EDAX) is carried out to identify the constituents of precipitates. Figure 7 displays the EDAX results and it is confirmed by EDAX analysis that all the precipitates are Al-Cu type. The left out precipitates in as-welded GTAW joint [Figure 7 a)] contain 5.2 % copper and 94.4 % aluminium. The undissolved precipitates of as-welded EBW joint contain 8 % copper and 92 % aluminium [Figure 7 b)]. The precipitates of as-welded FSW joint [Figure 7 c)] contain 14.7 % copper and 85.3 % aluminium. The precipitates of post-weld aged joints contain higher percentage of copper than the as-welded joints which is evident from EDAX results presented in Figures 7d) to f). The variation in composition of

Table 8 – Microhardness (HV) of the weld metal

Joint type	As-welded (AW) joint	Post weld aged (PWA) joint
BM	140	140
GTAW	90	100
EBW	105	117
FSW	110	124

precipitates is due to the difference in weld thermal cycles and post-weld ageing treatment.

Figure 8 displays the dislocation cell structure observed in the weld metal at very high magnification. The as-welded GTAW joint [Figure 8 a)] contains very widely spaced, less dense dislocation cell structure in the weld region. The as-welded EBW joint [Figure 8 b)] contains evenly spaced, less dense dislocation cell structure in the weld region. The as-welded FSW joint contains [Figure 8 c)] closely spaced, dense dislocation cell structure. The post weld aged joints [Figures 8 d)-f)] contain closely spaced, highly dense dislocation cell structure in the weld metal than their respective as-welded joints and this may be due to the movement of dislocations during post-weld ageing treatment.

4.5 Fracture surface

The fractographs of unnotched tensile specimens are displayed in Figure 9 and they invariably consist of dimples,

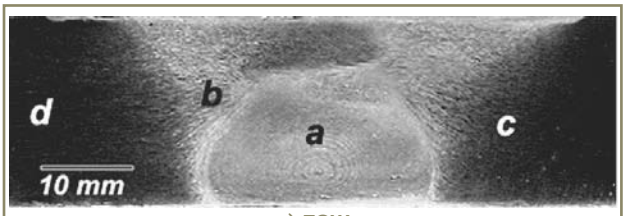

a) FSW

b) GTAW

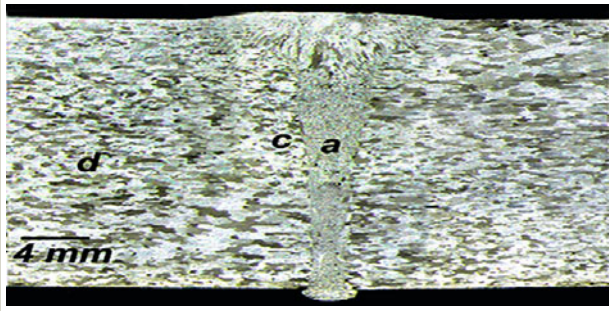

c) EBW

a) Weld metal region; b) Thermo-mechanically-affected zone; c) Heat-affected zone; d) Base metal.

Figure 4 – Cross-sectional macrostructure of welded joints

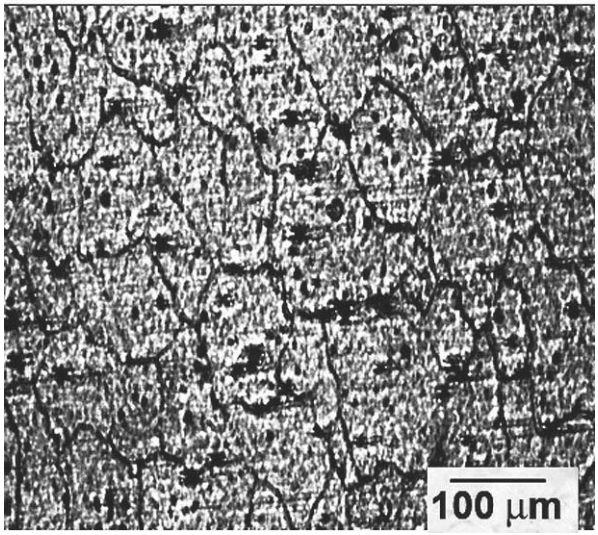

a) AW-GTAW

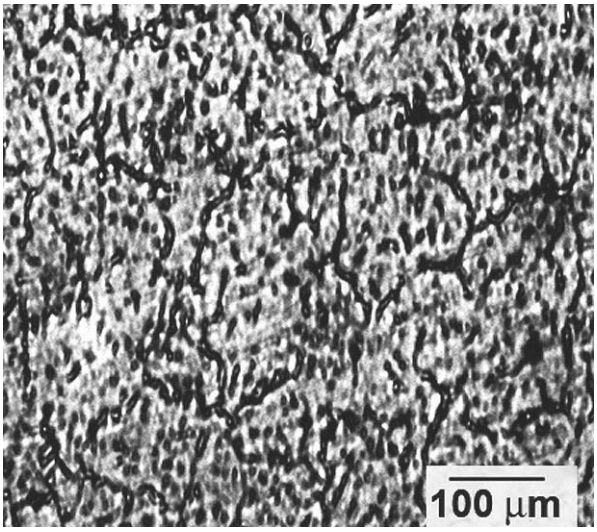

d) PWA-GTAW

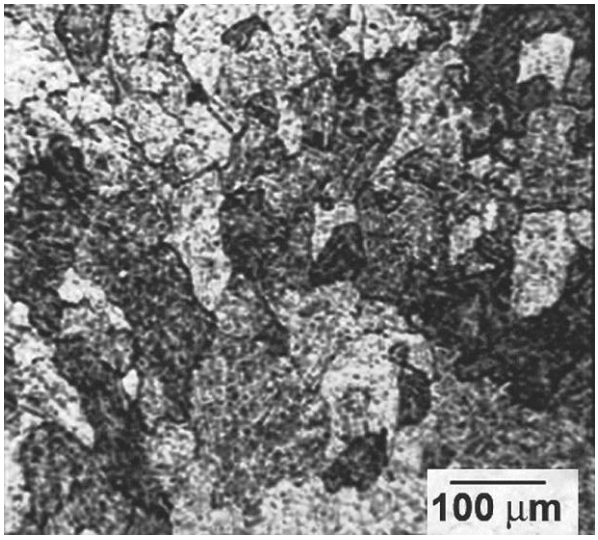

b) AW-EBW

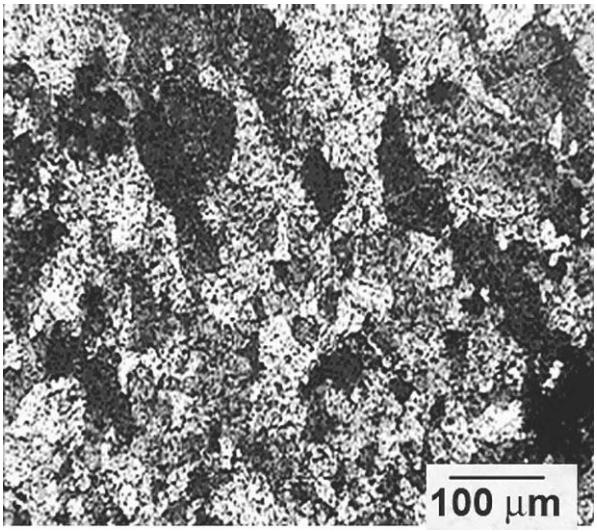

e) PWA-EBW

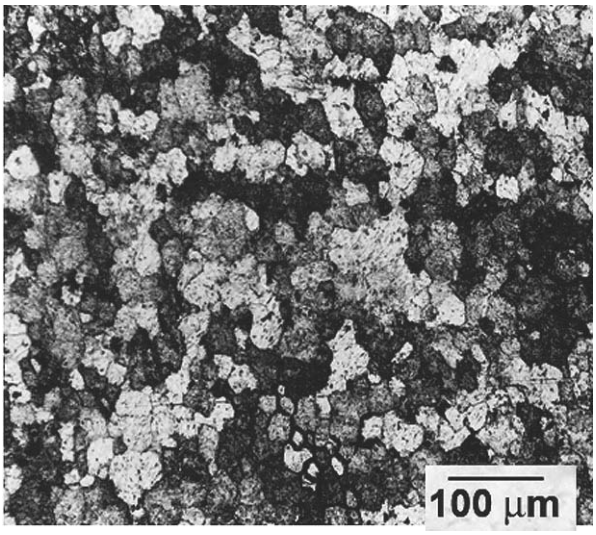

c) AW-FSW

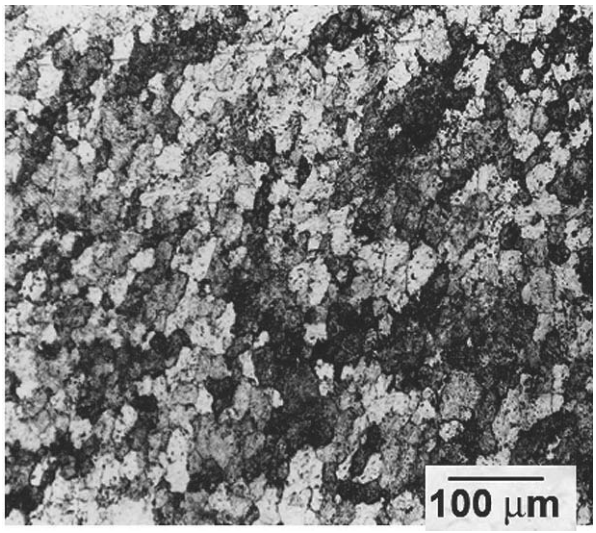

f) PWA-FSW

Figure 5 – Optical micrographs of weld metals

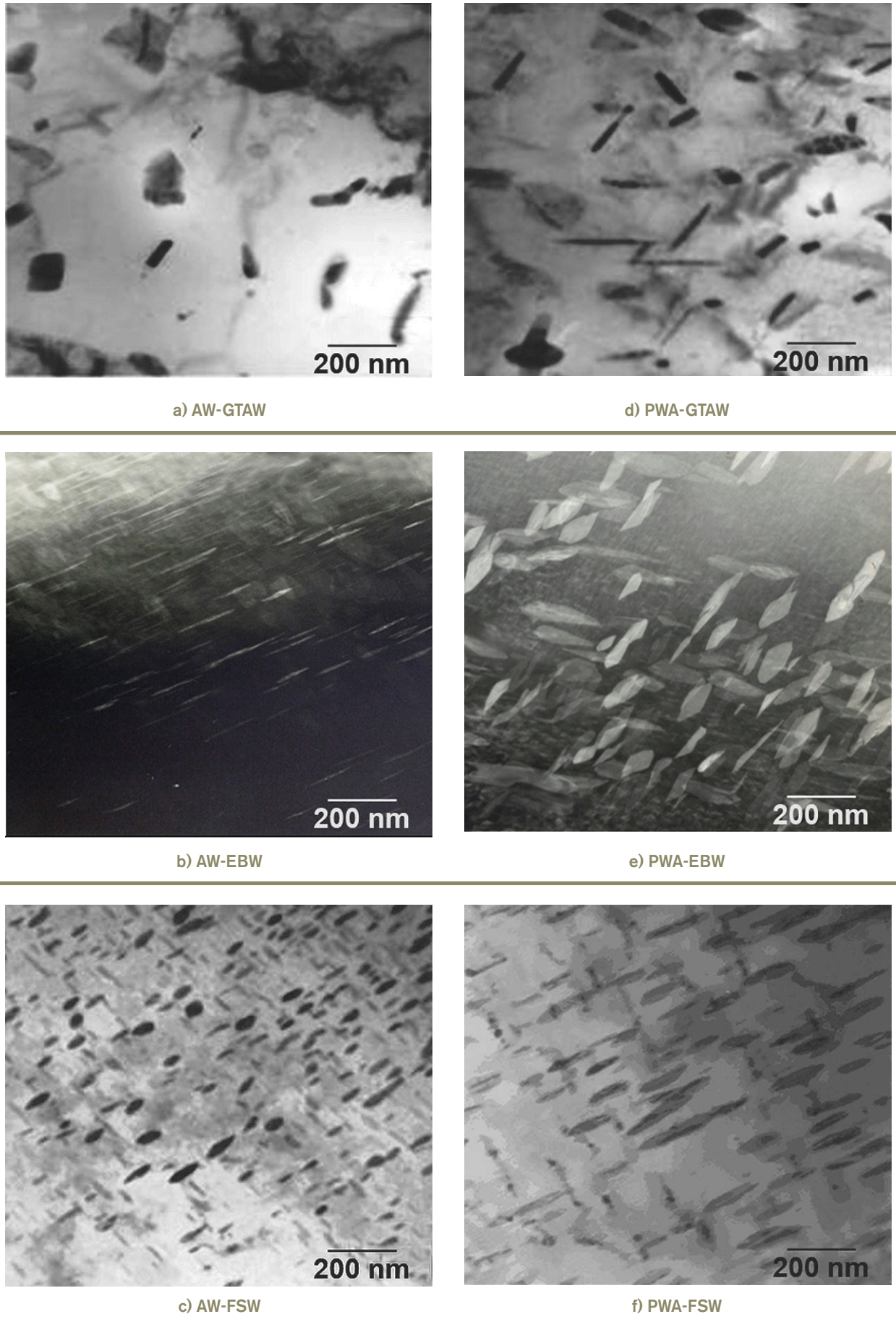

a) AW-GTAW

d) PWA-GTAW

b) AW-EBW

e) PWA-EBW

c) AW-FSW

f) PWA-FSW

Figure 6 – TEM micrograph of weld metal showing precipitates distribution

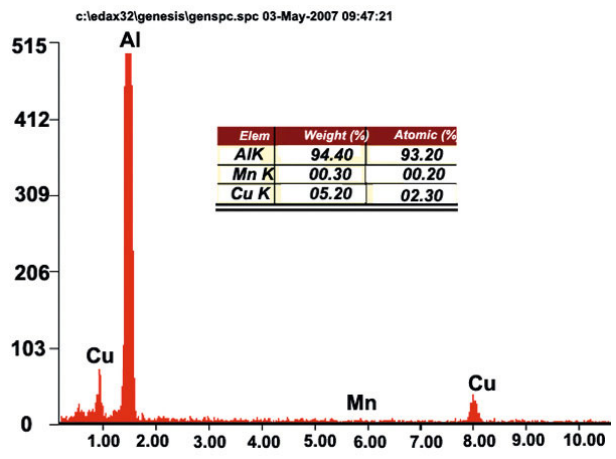

a) AW-GTAW

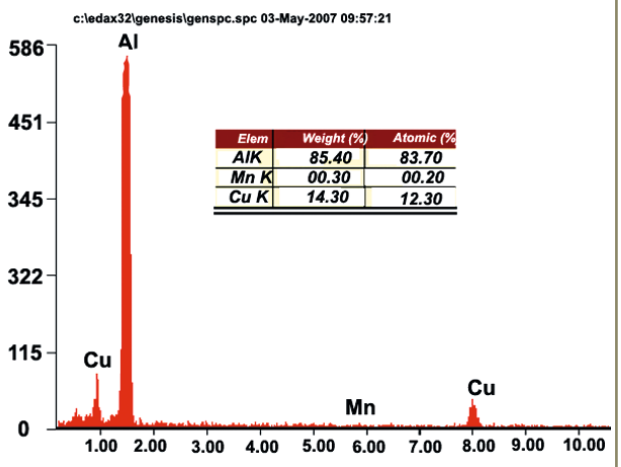

d) PWA-GTAW

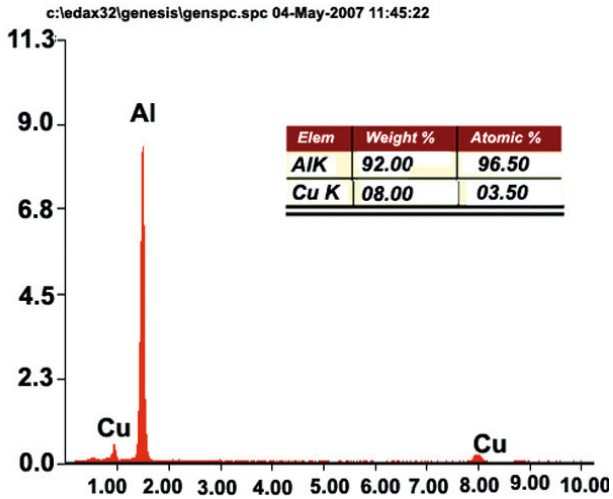

b) AW-EBW

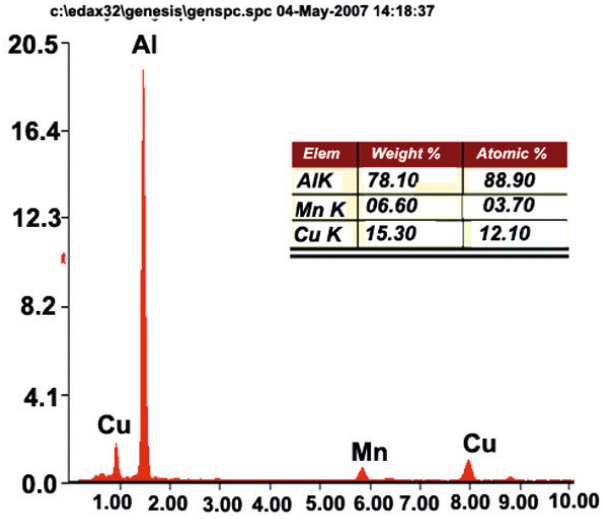

e) PWA-EBW

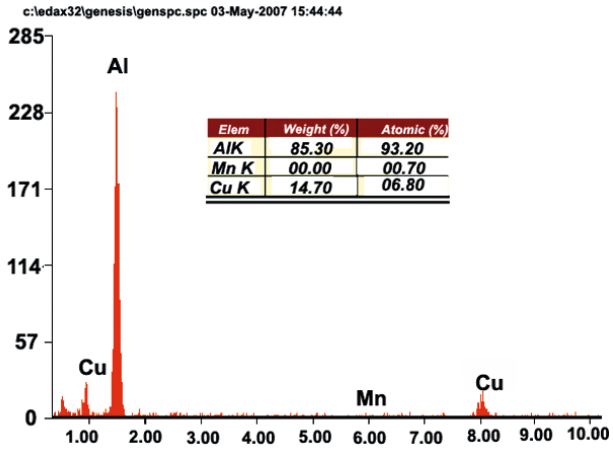

c) AW-FSW

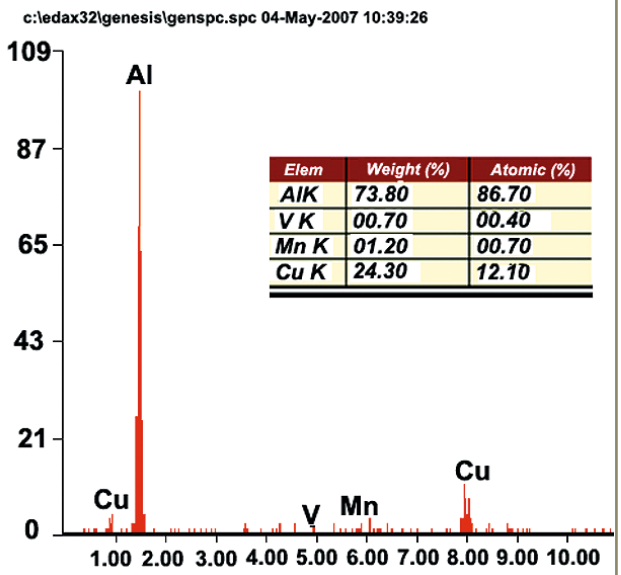

f) PWA-FSW

Figure 7 – EDAX results

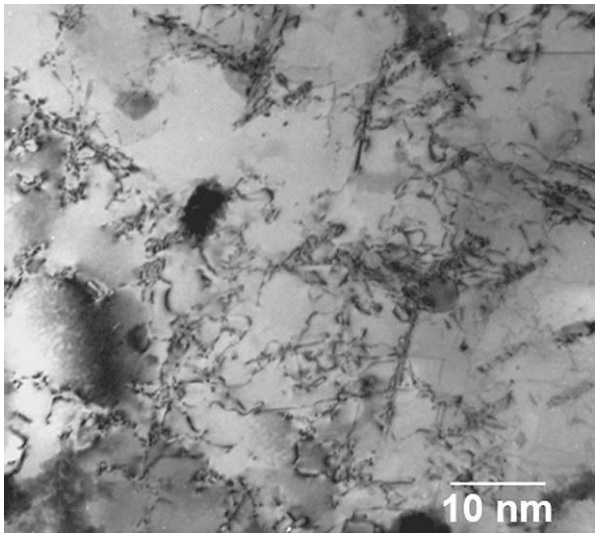

a) AW-GTAW

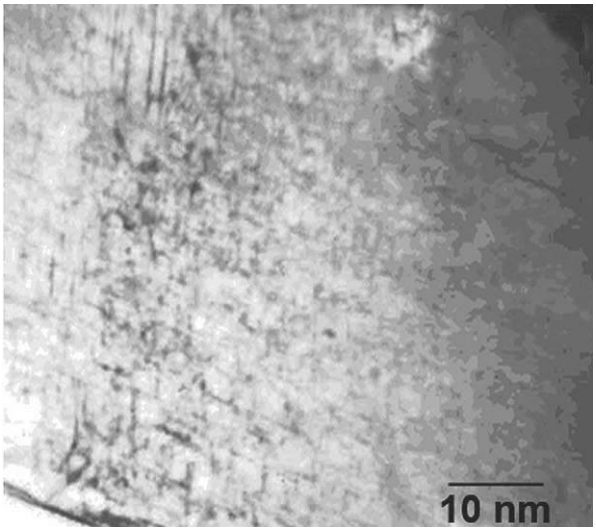

d) PWA-GTAW

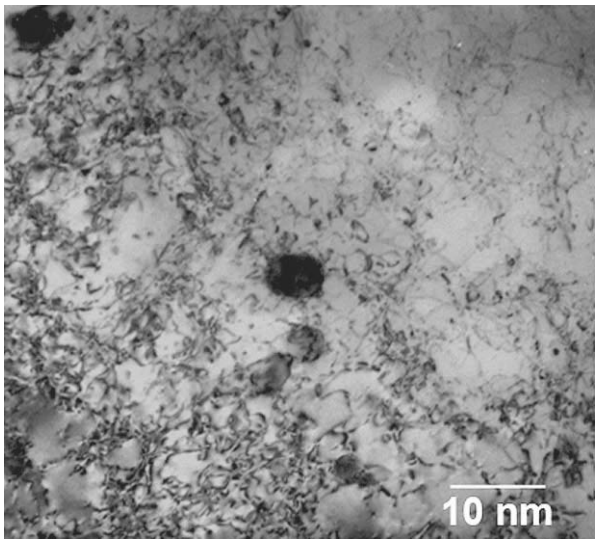

b) AW-EBW

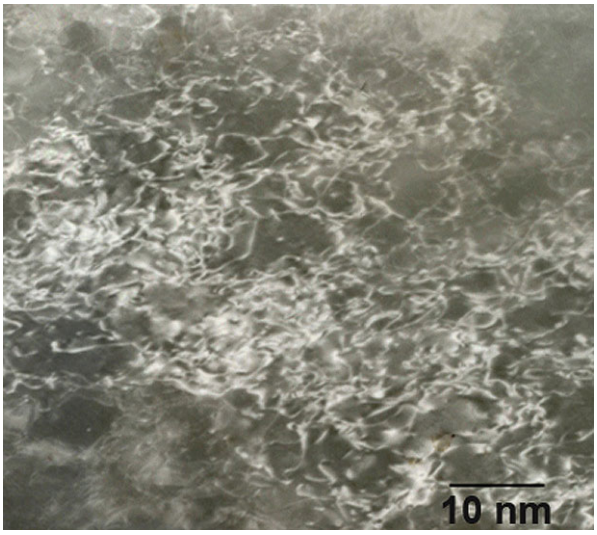

e) PWA-EBW

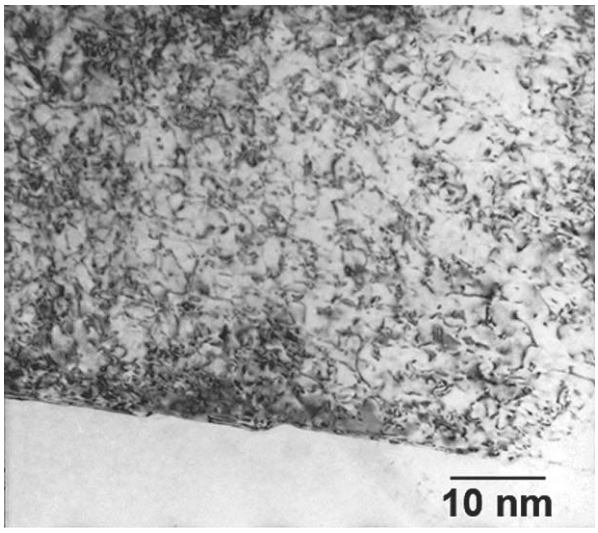

c) AW-FSW

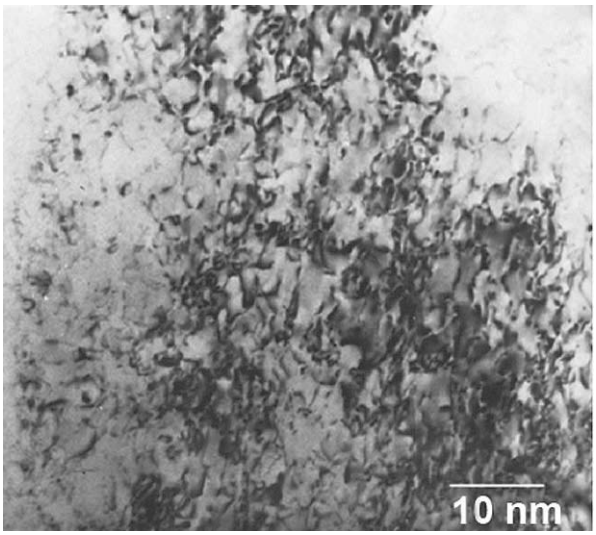

f) PWA-FSW

Figure 8 – TEM micrograph of weld metal showing dislocation cell structure

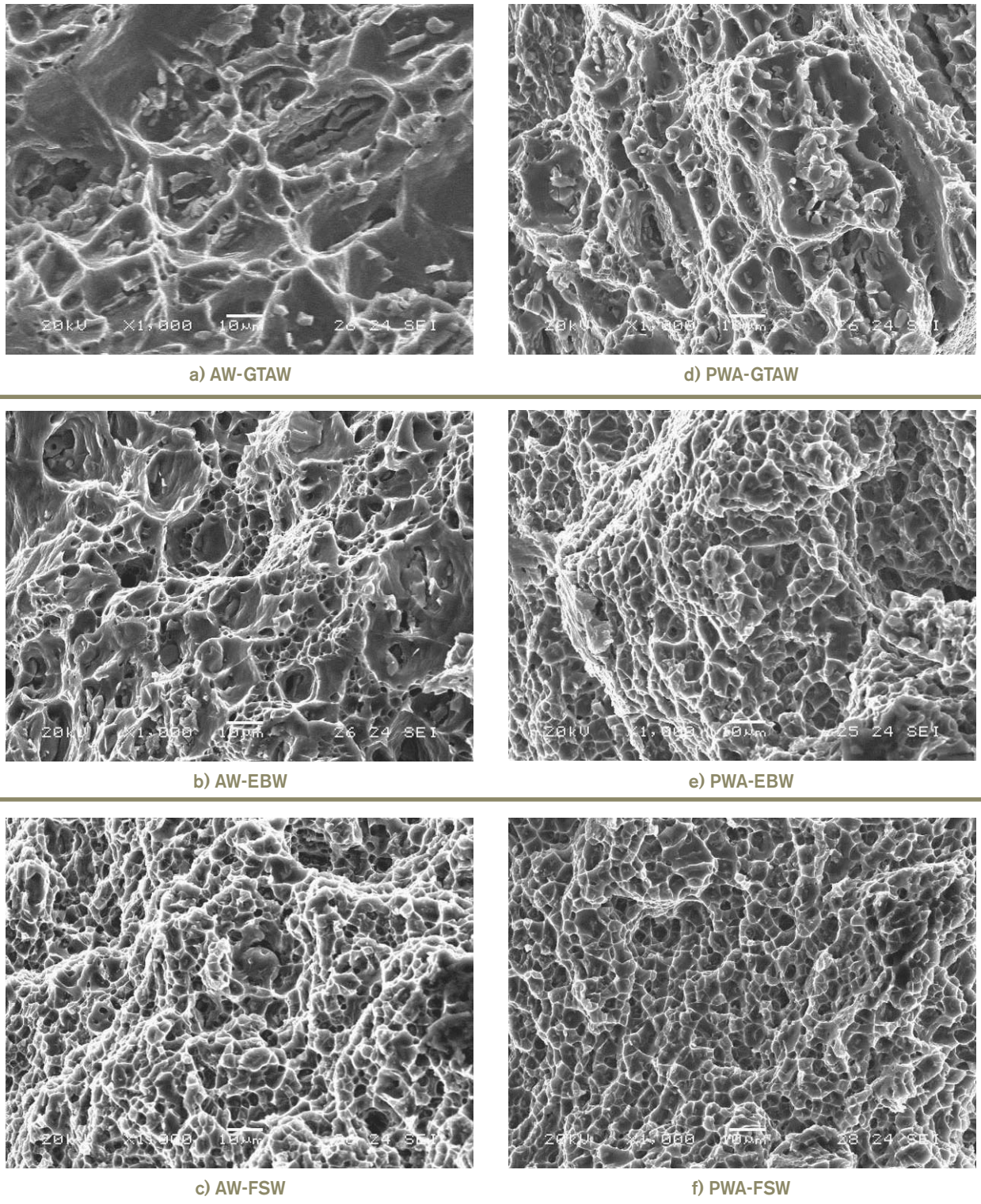

a) AW-GTAW

d) PWA-GTAW

b) AW-EBW

e) PWA-EBW

c) AW-FSW

f) PWA-FSW

Figure 9 – SEM fractograph of unnotched tensile specimens

which is an indication that the unnotched specimens failed in ductile manner under the action of tensile loading. Fine dimples are characteristic feature of purely ductile fracture and this feature validates that the specimen exhibits good ductility during tensile testing. Coarse and elongated dimples are seen in GTAW joint [Figures 9 a) and b)]. The elongated dimples are observed in EBW joint [Figures 9 c and d)]. However they are smaller when compared to GTAW joint. The dimples are finer in FSW joint [Figures 9 e) and f)] compared to other joints.

5 Discussion

Fine evenly distributed $CuAl_2$ precipitates are the reason for high strength of AA2219 base material. These strengthening precipitates form due to the solution treatment and subsequent artificial ageing. Though there is a possibility of formation of many precipitates, most of the precipitates are to be made up of Cu and Al [17]. Most of the tensile specimens (of welded joints) failed in the

weld metal region and it suggests that the weld metal region is weaker than the other regions. It is also evident from the hardness measurement (weld metal shows lower hardness than other regions). The size and distribution of $CuAl_2$ precipitates play a major role in deciding the tensile properties and hardness of the weld metal region of AA2219 alloy [8]. During GTA welding, these precipitates are assumed to dissolve and the weld metal should be left devoid of any precipitates [Figure 4 a)]. However, due to the high cooling rates involved in EB welding, all the precipitates do not dissolve only few of them get dissolved and few of them survive in a needle shaped precipitates throughout the matrix [Figure 4 b)]. But in FSW there is no melting and hence there is no dissolution of precipitates in the matrix. However, the precipitates are agglomerated due to stirring action of the rotating tool [Figure 4 c)].

GTAW joint resulted in precipitate free zone (PFZ) due to solutionizing of the weld metal by sufficient heat input caused by thermal cycle during welding. Since the PFZ is soft, strain concentration is extreme even though the macroscopic strain is very low [18]. This produces voids at the PFZ which then grow and coalesce along the PFZ leaving a coarse dimpled structure. Hence matrix of the GTA weld zone comprising precipitate free zone resulted in lowest hardness compared to EBW and FSW joints with corresponding poor tensile properties. GTA weld properties are controlled by the precipitate size and distribution. In the as-welded condition, solid solution strengthening is the primary strengthening mechanism. In the post-weld condition, an inhomogeneous distribution of solutes resulted in an inhomogeneous distribution of particles causing strain localization. The best overall weldment properties are obtained in the solution heat-treated and aged conditions, due to a homogeneous distribution of strengthening precipitates. The yield strength, ultimate tensile strength and elongation of the weldments increased with ageing treatments.

During EB welding, the rapid heating causes the weld metal and HAZ region to attain solution temperature. Since EB welding process is a faster process, the rate of cooling is higher (fast cooling) [19]. Hence, the AW condition itself resembles as solution treated (ST) condition. In the case of solution treatment, the material is directly quenched into cold water bath from solution temperature to retain the dissolved copper in the aluminium matrix itself. But in the as-welded condition, the joints are not quenched in cold water immediately after welding, instead, they are allowed to cool to room temperature [20]. Therefore, it is also possible that the precipitate particles in EB weld metal could have resulted from natural ageing of the weld metal after they have completely melted during welding process.

Bondarev [21] found that the coagulation of secondary phase particles in GTA welding is also the reason why it is not strong as the EB welded joints. There are no oxide film inclusions, no pores in EBW and structure in the HAZ is slightly changed; structural and chemical heterogeneity in fusion region are less. Hence tensile strength of the joint is 20 % greater than that of GTA welding. It was earlier shown by Vaidyanathan ***et al.***, [22] that at very early stages of precipitation the particles are rounded. Fine equiaxed grains in the friction stir weld metal implied that dynamic recrystallisation had taken place during FSW due to plastic deformation at elevated temperature. In heat treatable alloys, the static properties of the friction stir welds are dependent on the distribution of strengthening precipitates rather than the grain size [23]. The frictional heat and mechanical working of the plasticized material in the weld zone resulted in fine precipitates along with few needle shaped precipitates in the weld nugget which led to considerable hardening compared to GTAW and EBW joints. This increased the hardness of FSW joints considerably and exhibited higher tensile strength [24] than GTAW and EBW joints.

Not only the size and distribution of precipitates are influencing the hardness of the weld region, the composition of precipitates is also playing a major role in deciding the weld metal hardness [25]. The precipitates which are rich in copper content give better resistance to indentation and this is one of the reasons for higher hardness of post weld aged joints. The precipitates which are rich in aluminium content offer less resistance to indentation and this also another reason for lower hardness of as-welded joints.

The base metal usually contains closely spaced, dense dislocation cell structure and this is because of prior work hardening carried out on the material to attain T87 condition. Usually, very closely spaced, dense dislocation cell structure is an indication of amount of strain hardening the material undergone during prior metal working operations [26]. The formation of dislocation cell structure in the weld metal also influences the hardness of weld metal. The dislocation cell structure is disrupted in the weld metal (Figure 6a and 6b) due to the welding heat (wherever the exposure temperature is more than solution temperature). This is also another reason for lower hardness of as-welded joints of GTAW and EBW joints than FSW joints. However, the dislocation cell structure is not disrupted in FSW joint (Figure 6c) due to lower heat input (peak temperature is much lower than solution temperature). The post-weld ageing treatment carried out on the joints led to the reformation of dislocation cell structure in the weld metal of GTAW and EBW joints and this is evident from Figures 6 d) to e). Even though the cell structure is widely spaced, the reformation of dislocation cell enhanced the hardness of the weld metal and tensile properties of GTAW and EBW joints.

From the above results, it is very clear that the transverse tensile properties of AA2219 aluminium alloy have been greatly reduced by welding processes. Of the three welded joints, FSW joints showed better tensile properties compared to EBW and GTAW joints. Higher yield strength and tensile strength of the post weld aged FSW joint is greatly used to enhance the fatigue strength of these joints and hence the fatigue crack initiation is delayed. Larger elongation (higher ductility) of the post weld aged FSW joints also imparts greater resistance to fatigue

crack propagation and hence fatigue crack growth rate is comparatively slow. The combined effect of higher yield strength and higher ductility of the post weld aged FSW joint offers enhanced resistance to crack initiation and crack propagation and hence the fatigue performance of the these joints is superior compared to other joints. Similarly, the uniformly distributed, very fine particles throughout the matrix (weld region) might have impeded the growing fatigue cracks and hence the fatigue crack growth rate has been delayed [27] and subsequently the resistance to the fatigue crack propagation has been enhanced compared to other joints.

The magnitude of residual stress in the weld metal region of as-welded (AW) joints is usually tensile. This tensile residual stress field will be normally relieved, if artificial ageing treatment is carried out. Hence, in the post weld aged (PWA) joints, the magnitude of tensile residual stress field in the weld region will be much lower than the AW joints [28]. The higher magnitude of tensile residual stress, usually, will accelerate the speed of growing fatigue cracks. But in the post weld aged FSW joint, the magnitude of residual stress might be lower than as-welded joint. This may be the one of the reasons for the better fatigue performance of post weld aged FSW joints compared to other joints.

6 Conclusions

From this investigation following important conclusions are derived:

1. As-welded FSW joint exhibits the maximum joint efficiency of 72 % which is 40 % higher than GTAW joint and 12 % higher than EBW joint. As-welded FSW joint exhibits the maximum fatigue strength of 180 MPa which is 20 % higher than EBW joint and 50 % higher than GTAW joint.
2. Post-weld ageing treatment (PWA) was found to be beneficial to enhance the tensile strength and fatigue strength of as-welded (AW) joints, approximately 10-12 %. It is also beneficial to reduce the severity of notches under fatigue loading.
3. Post-weld aged FSW joint showed the highest tensile strength of 382 MPa and fatigue strength of 180 MPa and hence FSW process can be preferred over other welding processes to fabricate components and structures using AA2219 aluminium alloys.

Acknowledgements

The authors wish to record their sincere thanks to Aeronautical Research and Development Board (ARDB), New Delhi for the financial support to carryout this investigation through a R and D project No. DARO/08/1061356/M1. The authors are grateful to Mr. N. Viswanathan, Retired Scientist of Defence Research and Development Laboratory (DRDL), Hyderabad for providing EBW facility to carry out this investigation.

References

[1] Dance G.I.: Comparative evaluation of mechanical properties of TIG, MIG, EBW and VPPA welded AA2219 aluminum alloy, Welding Metal Fabrication, 2003, vol. 24, no. 1, pp. 216-222.

[2] Hartman J.A., Beil R.J., Hahn G.T.: Effect of copper rich regions on tensile properties of VPPA weldments of 2219-T87 aluminum, Welding Journal, 1987, vol. 32, no. 1, pp. 73-83.

[3] Tosto S., Nenci F., Hu J.: Microstructure and properties of Electron Beam welded and Post Welded 2219 Aluminium alloy, Material Science Technology 1996, vol. 12, no. 4, pp. 323-328.

[4] Ishchenko A., Ya A., Lozovskaya V., Sayenko I.M.I.: Fracture resistance of aluminium joints in high strength aluminium alloys under conditions of rapidly increasing load, Welding International, 1989, vol. 3, no. 8, pp. 654-656.

[5] Potluri N.B., Ghosh P.K., Gupta P.C., Reddy Y.S.: Studies on weld metal characteristics and their influences on tensile and fatigue properties of pulsed current GMA welded Al-Zn-Mg alloy, International Journal of Fatigue, 1997, vol. 19, no. 8, pp. 62-70.

[6] Kou S., Le Y.: Dendrite morphology in aluminium alloy welds, Metallurgical Transactions, 1983, vol. 14 A, no. 2, pp. 2243-2249.

[7] Huang C., Kou S.: Liquation cracking in full penetration Al-Cu welds, Welding Research Supplement, 2004, vol. 83, no. 1, pp. 50s-58s.

[8] Koteswara Rao S.R., Madhusudhana Reddy G., Srinivasa Rao K., Kamaraj M., Prasad Rao K.: Reasons for superior mechanical and corrosion properties of 2219 aluminum alloy electron beam welds, Materials Characterisation, 2005, vol. 55, no. 4-5, pp. 345-354.

[9] Liu H.J., Chen Y.C., and Feng J.C.: Effect of zigzag line on the mechanical properties of friction stir welded joints of an Al-Cu alloy, Scripta Materialia, 2006, vol. 55, no. 3, pp. 231-234.

[10] Xu W., Liu J., Luan G., and Don C.: Microstructure and mechanical properties of friction stir welded joints in 2219-T6 aluminium alloy, Material and Design, 2009, vol. 30, no. 9, pp. 3460-3467.

[11] Bala Srinivasan P., Arora K.S., Dietzel W., Pandey S., and Schaper M.: Characterisation of microstructure, mechanical properties and corrosion behavior of an

AA2219 friction stir weldment, Journal of Alloys and Compounds, 2010, vol. 492, no. 1-2, pp. 631-637.

[12] Dieter G.E.: Mechanical Metallurgy, 4th ed., Tata McGraw Hill, New York. 1988.

[13] Maddox S.J.: Review of fatigue assessment procedures for welded aluminium structures, International Journal of Fatigue, 2003, vol. 25, no. 12, pp. 359-1378.

[14] Hobbacher A.: Recommendations for the assessment of weld imperfections in respect to fatigue, 1988, IIW Doc. XIII-1266-88/XV 659-88, 1988.

[15] Jaccard R.: Fatigue crack propagation in aluminium, IIW Doc. XIII-1377-90, 1990.

[16] Sonsino C.M.: Fatigue assessment of welded joints in Al-Mg-4.5 Mn aluminium alloy AA 5083 by local approaches, International Journal of Fatigue, 1999, vol. 21, no. 9, pp 985-999.

[17] Garland J.G.: Weld pool solidification control, British Welding Journal, 1974, vol. 22, pp. 121-127.

[18] Becker D.W. and Adams C.M.: The role of pulsed GTA welding variables in solidification and grain refinement, Welding Journal, 1979, vol. 58, no.1, pp. 143s -149s.

[19] Ma T.: Softening behaviour of Al-Zn-Mg alloys due to welding, Material Science and Engineering A, 1999, vol. 266, no.1, pp. 198-204.

[20] Frazier W.E.: High-strength corrosion resistant aerospace aluminium alloys, Journal of Minerals, Metals and Materials Society, 2003, vol. 55, no.1, pp. 16-18.

[21] Bondarev A.A.: Electron beam welding of an Al-Cu-Mn alloy, Avt. Svarka., 1974, vol. 2, no.1, pp. 23-26.

[22] Vaidyanathan V., Wolverton C. and Chen L.Q.: Multiscale modeling of 'θ' precipitation in Al-Cu binary alloys, Acta Materialia, 2004, vol. 52, no. 10, pp. 2973-2987.

[23] Attallah M.M. and Salem H.G.: Friction stir welding parameters: a tool for controlling abnormal grain growth during subsequent heat treatment, Materials Science and Engineering A, 2005, vol. 391, no. 1-2, pp. 51-59.

[24] Bolderev.: Controlled solidification during fusion welding, Welding Production, 1977, vol. 18, no. 2, pp. 54-58.

[25] Gao M., C.R. Feng. and Wei, R.P.: An analytical electron microscopy study of constituent particles in commercial 7075-T6 and 2024-T3 alloys, Metallurgical and Materials Transactions A, 1998, vol. 29A, no. 2, pp. 1145-1151.

[26] Wei R.P., Liao C.M. and Gao M.: A transmission electron microscopy study of constituent particle-induced corrosion in 7075-T6 and 2024-T3 aluminium alloys, Metallurgical and Materials Transactions A, 1998, vol. 29, no. 4, pp. 1153-1160.

[27] Malarvizhi S., Raghukandan K. and Viswanathan N.: Effect of post weld heat treatment on fatigue behaviour of electron beam welded AA2219 aluminium alloy, Materials Design, 2008, vol. 29, no. 3-4, pp. 1562-1567.

[28] Malarvizhi S., Raghukandan K. and Viswanathan N.: Investigations on the effect of post weld heat treatment on fatigue crack growth behaviour of electron beam welded AA2219 aluminium alloy, International Journal of Fatigue, 2008, vol. 30, no. 9, pp. 1543-1555.

About the authors

Dr. Sudersenan MALARVIZHI (jeejoo@rediffmail.com) and Dr. Visvalingam BALASUBRAMANIAN (visvabalu@yahoo.com) are both with the Centre for Materials Joining and Research (CEMAJOR), Department of Manufacturing Engineering, Annamalai University,Tamil Nadu (India).